

Energy Harvesting WSNs for Accurately Estimating the Maximum Sensor Reading: Trade-Offs and Optimal Design

Shilpa Rao and Neelesh B. Mehta, *Senior Member, IEEE*

Abstract—Computing the maximum of sensor readings arises in several environmental, health, and industrial monitoring applications of wireless sensor networks (WSNs). We characterize the several novel design trade-offs that arise when green energy harvesting (EH) WSNs, which promise perpetual lifetimes, are deployed for this purpose. The nodes harvest renewable energy from the environment for communicating their readings to a fusion node, which then periodically estimates the maximum. For a randomized transmission schedule in which a pre-specified number of randomly selected nodes transmit in a sensor data collection round, we analyze the mean absolute error (MAE), which is defined as the mean of the absolute difference between the maximum and that estimated by the fusion node in each round. We optimize the transmit power and the number of scheduled nodes to minimize the MAE, both when the nodes have channel state information (CSI) and when they do not. Our results highlight how the optimal system operation depends on the EH rate, availability and cost of acquiring CSI, quantization, and size of the scheduled subset. Our analysis applies to a general class of sensor reading and EH random processes.

Index Terms—Energy harvesting, wireless sensor networks, max function computation, fading, quantization.

I. INTRODUCTION

BATTERY-OPERATED wireless sensor networks (WSNs) are finding increasing acceptance in a diverse range of applications such as military surveillance, health, and home automation [1]. Low cost, avoidance of power cables, and ease of deployment have made them popular.

One appealing application of WSNs involves determining the maximum of the sensor readings in the network [2]–[5]. It is motivated by applications like early detection of an impending event such as a fire and determining the highest level of pollution in environmental monitoring. It also serves as a trigger for further action in a monitoring and control loop. This is because if the maximum is below a threshold, then it implies that no reading exceeds the threshold. It is an instance

of network function computation in WSNs, which aims to efficiently aggregate data and not just transport it [2]–[4], [6].

As sensor nodes consume energy when they operate and deplete their batteries over time, several techniques that extend the lifetime of WSNs [7] or the rate at which they aggregate data have been studied. These include block computation [3], opportunistic selection [5], and in-network filtering [8]. Energy harvesting (EH) is a green alternate solution to address this problem. EH sensor nodes equipped with rechargeable energy buffers, such as batteries or supercapacitors, harvest energy from renewable sources such as solar, vibration, and wind, and replenish their energy buffers [9]–[11].

While EH can ensure perpetual operability of the WSN, new challenges arise due to the randomness in the harvested energy. Specifically, in max function computation, the fusion node (FN) may occasionally fail to determine the maximum if the node with the max reading fails to transmit data to the FN due to low energy or a bad channel condition. In general, this is determined by the EH and channel fading processes, data arrivals, protocols, and channel state information (CSI).

Focus and Contributions: In this paper, we highlight, analyze, and optimize the several novel system design trade-offs that arise in designing EH WSNs for max function computation. We study an EH WSN with a star topology [3], [12]–[15]. Time is divided into data collection rounds (DCRs). The FN estimates the max sensor reading in each DCR. This is called the one-shot computation paradigm in the literature [2], [4]. In every DCR, a subset of the nodes is scheduled to transmit as per a pre-defined *transmission schedule*. The channels between the nodes and the FN undergo fading, due to which some transmissions may not be decoded by the FN.

We analyze the mean absolute error (MAE), which is defined as the expected value of the absolute difference between the maximum sensor reading in the WSN and that estimated by the FN in a DCR. The smaller the value of the MAE, the better is the performance of the WSN. For a randomized transmission schedule in which a pre-specified number of K randomly selected sensor nodes are scheduled to transmit in a DCR, we derive closed-form expressions for the minimum MAE and the optimal transmit power given any K . We then optimize K itself. The randomized transmission schedule is fair because all the nodes get, on average, equal opportunity to transmit their readings, and is tractable.

We first analyze the base model in which the nodes have no CSI during transmission and characterize the following

Manuscript received August 1, 2014; revised January 5, 2015; accepted April 1, 2015. Date of publication April 14, 2015; date of current version August 10, 2015. A part of this paper has been presented at IEEE GlobalSIP 2014. This research is partly supported by a research grant from ANRC. The associate editor coordinating the review of this paper and approving it for publication was L. Lai.

The authors are with the Department of Electrical Communication Engineering, Indian Institute of Science (IISc), Bangalore 560 012, India (e-mail: devashilpa@gmail.com; nbmehta@ece.iisc.ernet.in).

Digital Object Identifier 10.1109/TWC.2015.2422811

two fundamental trade-offs. Increasing the transmit energy or making more nodes transmit in a DCR improves the estimate of the maximum in that DCR, but it also drains more energy from the nodes, which reduces the odds that the nodes will have sufficient energy to transmit later. Thereafter, we analyze the alternate model in which nodes have CSI and, therefore, save energy by not transmitting if their channel is in a deep fade. However, acquiring CSI itself requires energy. Our results characterize when acquiring CSI is beneficial.

Finally, we study and similarly optimize a more practical scenario in which the nodes transmit quantized readings to the FN, and characterize the following additional trade-off. While using more bits reduces the quantization error in estimating the maximum, it also consumes more energy, which can curtail subsequent transmissions. A trade-off between the number of bits and K also arises. We determine the optimal transmit power, optimal number of scheduled nodes, and quantization bits that jointly minimize the MAE.

The results hold for any stationary and ergodic sensor reading processes in which the readings have continuous distributions with positive support, and for the general class of all stationary and ergodic EH processes, which covers a wide variety of models studied in the literature [9], [10], [14]. Insightful simplifications for specific statistical models of the sensor readings are also presented. Altogether, our model and its results capture various important aspects of wireless communications and EH WSN design. It is different from the estimation models in EH literature, which we discuss below.

Related EH Literature and Comparisons: Though [13], [16]–[18] deal with estimation error minimization in EH WSNs, the trade-offs and error minimization in max function computation in EH WSNs are not studied. For a single EH node network, [16] optimizes the transmit power to minimize the mean squared error (MSE). In [13], for a multi-node WSN, the optimal transmit energy that minimizes the maximum MSE over a finite time period is determined. In [17], an iterative algorithm is proposed to estimate the intensity of spatially correlated vibrations that are measured by EH nodes. In [18], the nodes observe a set of common processes and transmit their observations to the FN. A power allocation policy that minimizes the average transmit power and the average battery backup unit usage subject to an MSE constraint is derived.

Outline: The system model is presented in Section II. We minimize the MAE for unquantized measurements in Section III and for quantized measurements in Section IV. Numerical results in Section V are followed by our conclusions in Section VI.

Notation: We use the following notation henceforth. The probability of an event A is denoted by $\Pr(A)$. For a random variable (RV) X , its expected value is denoted by $\mathbb{E}[X]$. The cumulative density function (CDF) and the probability density function (PDF) of a RV X are denoted by $F_X(\cdot)$ and $f_X(\cdot)$, respectively. The floor of a real number x is denoted by $\lfloor x \rfloor$. $W_0(x)$, for $x \geq -1$, denotes the principal branch of the Lambert W-function [19]. For N RVs X_1, X_2, \dots, X_N , $X_{r:N}$ denotes the r^{th} smallest value [20, Chapter 1]. Clearly, $X_{1:N} \leq X_{2:N} \leq \dots \leq X_{N:N}$. $x \rightarrow x_0^-$ and $x \rightarrow x_0^+$ denote x approaching x_0 from the left and right sides, respectively.

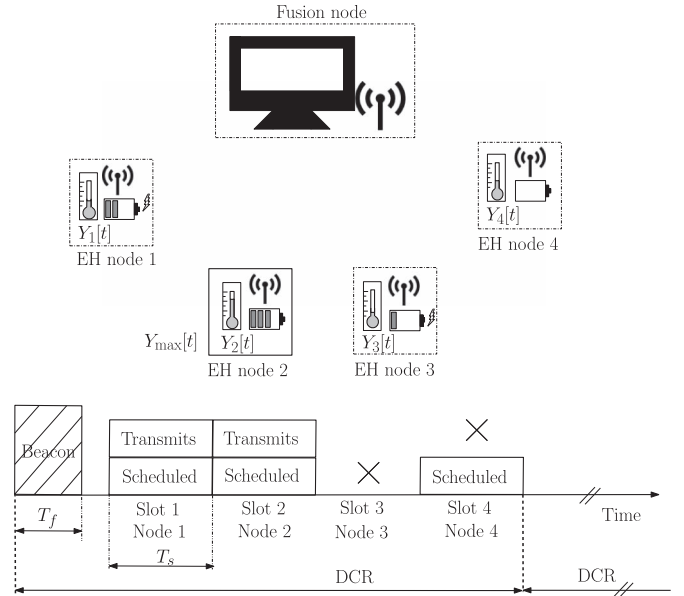


Fig. 1. Illustration of an EH WSN consisting of $N = 4$ EH nodes that transmit data to the FN over time-varying wireless links that undergo fading, and the events that might occur when $K = 3$ nodes are scheduled in a DCR.

II. SYSTEM MODEL

As shown in Fig. 1, we consider a WSN with N EH nodes and an FN. The sensor readings, the energy buffer evolution, and channel fading random processes are modeled as follows.

Sensor Readings: Each DCR is of duration T_{rd} . The DCR duration is driven by the sensing application, and is a function of how often the readings need to be conveyed to the FN. Let $Y_i[t]$ denote the real-valued sensor reading at the i^{th} node in the t^{th} DCR. These readings remain unchanged within a DCR. However, they can change across DCRs. As mentioned, we assume $Y_i[t] \geq 0$, for $t \geq 1$ and $1 \leq i \leq N$. This arises in practice in measuring quantities such as energy of vibrations, chemical concentrations, or temperatures. Further, we assume that $Y_i[t]$ are stationary and ergodic and identically distributed across DCRs [12], [16] and nodes. However, they can be correlated across nodes or time. For example, the temperature readings of close-by nodes can be highly correlated. The maximum reading $Y_{\max}[t]$ in the t^{th} DCR is equal to

$$Y_{\max}[t] = \max \{Y_1[t], Y_2[t], \dots, Y_N[t]\}. \quad (1)$$

EH and Storage Model: Each node has a finite start-up energy in its energy buffer. The capacity of the energy buffer is infinite [13], [21]. The EH process at a node is assumed to be stationary and ergodic with mean $\bar{H} > 0$ per DCR, and is independent and identically distributed (i.i.d.) across nodes. The energy harvested in a DCR is available for use in subsequent DCRs [10], [14].

Channel Model: Let $h_i[t]$ denote the frequency-flat channel power gain of the i^{th} EH node in the t^{th} DCR. This channel model holds when the signal bandwidth is less than the coherence bandwidth [22]. This model is used when maximizing the data rate is not the main goal [23]. We assume Rayleigh fading. Furthermore, $h_i[t]$, for $1 \leq i \leq N$ and $\forall t$, are assumed

to be i.i.d. [14], [23] for analytical tractability. Let γ_0 denote the mean channel power gain, which includes the path-loss.

Transmission Model: Let T_{int} denote the time allocated for transmissions in a DCR. In each DCR, as per a pre-specified transmission schedule, K nodes transmit their data sequentially in slots of duration $T_s = T_{\text{int}}/N$ each. When $K = N$, this model reduces to the simpler one in [13]. Our model corresponds to the widely studied time division multiple access (TDMA) media access control (MAC) protocol [14], [24] and is employed in standards such as Wireless HART (Highway Addressable Remote Transducer) [25] and ISA-100.11a [26]. TDMA reduces collisions, contention overheads, and can reduce latency. We do not explicitly model the control messages that are exchanged to initially set up the network. In effect, the energy incurred in this initial exchange is assumed to be negligible as it can be amortized over many DCRs.

Let the transmit power of a node be P . We study the fixed power model as it enables energy-efficient power amplifier design [14], [27]. As the channel gains of different nodes are statistically identical, the average signal-to-noise-ratio (SNR) at the FN is the same for all the nodes. The FN decodes the transmission of node i at time t if the SNR $h_i[t]P/(\eta k_B \Delta W)$ exceeds a threshold ω , where η is the noise figure, k_B is Boltzmann's constant, Δ is the temperature in Kelvin, and W is the bandwidth. The channel between node i to the FN is said to be *good* if $h_i[t] \geq \omega \eta k_B \Delta W / P$. As mentioned, the transmission schedule is not a function of the instantaneous energy in the energy buffers or the channel gains, as this information is local to the nodes. Communicating it to the FN to optimize the efficacy of the schedule entails significant energy, time, and protocol-related overheads.

How a node transmits depends on the CSI it has. Hence, we consider the following models:

- i) *With-CSI model:* In the beginning of every DCR, the FN broadcasts a beacon for a duration T_f . A node expends cT_f energy, where c is the power consumed for reception, to receive the beacon and estimate its channel. A node scheduled to transmit in a DCR estimates its channel only if it has energy $cT_f + PT_s$ in its energy buffer for both CSI acquisition and transmission. A node transmits only if its estimated channel gain is good. For analytical simplicity, we shall assume that the channel estimation error is negligible [13], [24].
- ii) *Without-CSI model:* Unlike the with-CSI model, the nodes do not estimate their channels. Hence, they do not spend energy on channel estimation. A node's decision to transmit does not depend upon its channel gain. Hence, a scheduled node transmits if it has energy PT_s in its energy buffer.

When a scheduled node does not transmit in its slot or if its transmission is not decoded by the FN, which can happen in the without-CSI model, the FN sets the measurement reported in this slot to be zero as this does not affect the maximum calculated from the other received measurements.

Measurement Error: Let \mathcal{S}_t denote the set of nodes whose measurements are received and decoded by the FN in DCR t .

Let $Y_{\text{meas}}[t]$ denote the maximum of the measurements received by the FN in the t^{th} round. Then,

$$Y_{\text{meas}}[t] = \begin{cases} \max_{i \in \mathcal{S}_t} Y_i[t], & \mathcal{S}_t \neq \phi, \\ 0, & \mathcal{S}_t = \phi, \end{cases} \quad (2)$$

where ϕ denotes the null set. The absolute measurement error $\chi[t]$ in the t^{th} round is

$$\chi[t] = |Y_{\text{max}}[t] - Y_{\text{meas}}[t]| = Y_{\text{max}}[t] - Y_{\text{meas}}[t]. \quad (3)$$

III. MAE MINIMIZATION

We analyze the MAE of the system in steady state, and shall assume that such a steady state exists. By steady state, we mean the regime in which the probability distribution of the state variables has become stationary. The randomness in the EH, fading, and scheduling processes, and energy buffers is still captured by this assumption. We henceforth drop the time index t and consider the system in an arbitrary DCR.

We want to find the optimal K and P that give the infimum (inf) of MAE:

$$\begin{aligned} & \inf_{P, K} \mathbb{E}[\chi] \\ & \text{s. t. } P \geq 0 \text{ and } 1 \leq K \leq N. \end{aligned} \quad (4)$$

We solve this optimization problem in two stages. Firstly, for any given K , we determine the infimum of the MAE, which is denoted by $\bar{\chi}_K^*$, in closed-form. Further, we show that the infimum is achievable. Thus, $\bar{\chi}_K^*$ is the minimum MAE for a given K . Thereafter, we numerically find the optimal K , denoted by K^* , in Section V.

Theorem 1: In the without-CSI model, $\bar{\chi}_K^* = \mathbb{E}[Y_{N:N}] - \mathcal{Y}_1$, where

$$\mathcal{Y}_1 = \begin{cases} \frac{\bar{H}}{K\xi e} \sum_{l=1}^K \mathbb{E}[Y_{l:K}] \left(1 - \frac{\bar{H}}{K\xi e}\right)^{K-l}, & 0 < \bar{H} < K\xi, \quad (5a) \\ e^{-\frac{K\xi}{\bar{H}}} \sum_{l=1}^K \mathbb{E}[Y_{l:K}] \left(1 - e^{-\frac{K\xi}{\bar{H}}}\right)^{K-l}, & \bar{H} \geq K\xi, \quad (5b) \end{cases}$$

and $\xi = \omega \eta k_B \Delta W T_s / (N \gamma_0)$.

The optimal transmit power P_K^* that achieves it is given by

$$P_K^* = \begin{cases} \frac{N\xi}{T_s}, & 0 < \bar{H} < K\xi, \quad (6a) \\ \frac{N\bar{H}}{KT_s}, & \bar{H} \geq K\xi. \quad (6b) \end{cases}$$

Proof: The proof is relegated to Appendix A. ■

Insights: First, we see that ξ is a key constant that governs the optimal power and the minimum MAE. It is the ratio of the SNR threshold ω to the average SNR $\gamma_0/(\eta k_B \Delta W T_s)$ if a node were to transmit with unit energy for a duration T_s . The ratio is further scaled down by the number of EH nodes N . Second, in both (5a) and (5b), the order statistics of the l^{th} smallest value among K RVs is scaled with the probability that it is the highest measured sensor reading in the DCR. Third, we see that the behavior of the EH WSN is different under two different

regimes. In the first regime $0 < \bar{H} < K\xi$, the nodes are energy-starved and the optimal transmit power is independent of the harvested energy (cf. (6a)). In the second regime, the nodes are energy-rich and the optimal transmit power increases as \bar{H} increases (cf. (6b)). Also, P_K^* depends only on the mean of the EH and channel fading processes.

$\mathbb{E}[Y_{l:K}]$ depends on the statistics of the sensor readings. To gain more insights, we study the following two examples:

- i) Y_1, Y_2, \dots, Y_N are independent and uniformly distributed in the interval $[0,1]$: Here, $\mathbb{E}[Y_{l:K}] = l/(K+1)$ and $\mathbb{E}[Y_{N:N}] = N/(N+1)$. The minimum MAE with K nodes simplifies to

$$\bar{\chi}_K^* = \begin{cases} \frac{K\xi e}{\bar{H}(K+1)} - \frac{1 + \frac{K\xi e}{\bar{H}}}{K+1} \left(1 - \frac{\bar{H}}{K\xi e}\right)^K - \frac{1}{N+1}, & 0 < \bar{H} < K\xi, \\ \frac{K\xi}{e^{\frac{K\xi}{\bar{H}}}} - \frac{1 + e^{-\frac{K\xi}{\bar{H}}}}{K+1} \left(1 - e^{-\frac{K\xi}{\bar{H}}}\right)^K - \frac{1}{N+1}, & \bar{H} \geq K\xi. \end{cases}$$

- ii) Y_1, Y_2, \dots, Y_N are independent and exponentially distributed with mean λ : Here, $\mathbb{E}[Y_{l:K}] = \lambda \sum_{j=K-l+1}^K 1/j$ and $\mathbb{E}[Y_{N:N}] = \lambda \sum_{j=1}^N 1/j$.

The minimum MAE with K nodes is

$$\bar{\chi}_K^* = \begin{cases} \lambda \sum_{j=1}^N \frac{1}{j} - \frac{\bar{H}\lambda}{K\xi e} \sum_{y=1}^K \left(1 - \frac{\bar{H}}{K\xi e}\right)^y \sum_{z=K-y+1}^K \frac{1}{z}, & 0 < \bar{H} < K\xi, \\ \lambda \sum_{j=1}^N \frac{1}{j} - \lambda e^{-\frac{K\xi}{\bar{H}}} \sum_{y=1}^K \left(1 - e^{-\frac{K\xi}{\bar{H}}}\right)^y \times \sum_{z=K-y+1}^K \frac{1}{z}, & \bar{H} \geq K\xi. \end{cases}$$

Note that when the MAE is normalized with respect to $\mathbb{E}[Y_{N:N}]$, it turns out to be independent of λ .

Theorem 2: Define $\Omega_1 = W_0 \left(\frac{KN\xi}{N\bar{H} - KcT_f} \right)$ and $\Omega_2 = W_0 \left(\frac{1}{2} \sqrt{\frac{N\xi}{cT_f}} \right)$. In the with-CSI model, $\bar{\chi}_K^* = \mathbb{E}[Y_{N:N}] - \mathcal{I}_2$, where

$$\mathcal{I}_2 = \begin{cases} \sigma_1 \sum_{l=1}^K \mathbb{E}[Y_{l:K}] (1 - \sigma_1)^{K-l}, & \bar{H} \geq \frac{KcT_f}{N} \text{ and } \Omega_1 \leq 2\Omega_2, \\ \sigma_2 \sum_{l=1}^K \mathbb{E}[Y_{l:K}] (1 - \sigma_1)^{K-l}, & \text{otherwise,} \end{cases} \quad (7a)$$

$$\sigma_1 = \frac{(N\bar{H} - KcT_f)\Omega_1}{KN\xi}, \text{ and } \sigma_2 = \frac{4\bar{H}\Omega_2^2}{K\xi + 2K\xi\Omega_2^2}.$$

The optimal transmit power P_K^* that achieves it is given by

$$P_K^* = \begin{cases} \frac{N\xi}{T_s\Omega_1}, & \bar{H} \geq \frac{KcT_f}{N} \text{ and } \Omega_1 \leq 2\Omega_2, \\ \frac{N\xi}{2T_s\Omega_2}, & \text{otherwise.} \end{cases} \quad (8a)$$

$$P_K^* = \begin{cases} \frac{N\xi}{T_s\Omega_1}, & \bar{H} \geq \frac{KcT_f}{N} \text{ and } \Omega_1 \leq 2\Omega_2, \\ \frac{N\xi}{2T_s\Omega_2}, & \text{otherwise.} \end{cases} \quad (8b)$$

Proof: The proof is relegated to Appendix B. ■

Notice the critical role played by the constants Ω_1 and Ω_2 , which are, in turn, determined by the system parameters c , T_f , ξ , N , and K . As before, in the energy-starved regime, P_K^* is a constant. And, it increases once \bar{H} exceeds a certain threshold, which is a function of the size of the scheduled subset, the CSI acquisition cost, and the number of EH nodes in the WSN. In both Theorems 1 and 2, P_K^* is independent of the distribution

of the sensor readings. For the uniform and exponentially distributed independent sensor readings examples above, the corresponding MAE expressions are not shown to conserve space.

Comment: The steady state analysis that we use is a natural engineering tool for studying EH systems that focus on perpetual network operation. We have empirically verified that our system reaches steady state for various EH models of interest. The energy buffer evolution of any node in our system can be shown to be closely linked to the workload process of the $G/G/1$ queue, which is described by the Lindley equation [28]. Hence, the Loynes' stability criteria can be applied to our system. From it, for the without-CSI model, we find that when $\bar{H} > KP T_s/N$, the energy buffer of a node tends to infinity almost surely, and $Y_{\text{meas}}[t]$, which now depends on the sensor readings, channel fading, and scheduling processes, becomes stationary. When $\bar{H} < KP T_s/N$, the energy buffer of a node can be shown to be stable. The case when $\bar{H} = KP T_s/N$ is avoided in practice by slightly reducing $P T_s$, which pushes the system to a steady state. Similar analogies exist for the other models. Also, in [21], existence of steady state is proved for an i.i.d. EH process and fixed power transmission.

IV. MAE WITH QUANTIZED MEASUREMENTS

In practice, nodes transmit quantized data as the bandwidth is limited. This introduces a quantization error in the MAE, and a new design trade-off arises, which we study below.

Quantization Model: Let \hat{Y}_i denote the q -bit quantized value of Y_i . Clearly, \hat{Y}_i can take 2^q different values. Let $[v_{j-1}, v_j]$, for $1 \leq j \leq 2^q$, be the quantization regions, where v_0 and v_{2^q} are the left and the right limits of the support set of Y_i . When $Y_i \in [v_{j-1}, v_j]$, $\hat{Y}_i = v_{j-1}$. Let \hat{Y}_{meas} denote the maximum of the quantized measurements received by the FN.

$$\hat{Y}_{\text{meas}} = \begin{cases} \max_{i \in S} \hat{Y}_i, & S \neq \phi, \\ 0, & S = \phi. \end{cases} \quad (9)$$

Transmission Model: Let R be the transmit data rate. Then, for a practical code, the minimum SNR ω at which a transmission can be decoded is

$$\omega = \left(2^{\frac{R}{W}} - 1\right) \frac{1}{\alpha}, \quad (10)$$

where $\alpha \in (0, 1]$ is the coding loss of the code [22]. The time required to transmit a q -bit reading is q/R and at most $\lfloor RT_s \rfloor$ bits can be transmitted in a slot of duration T_s . Unlike Section III, here only a fraction of the slot duration, which depends on q , is used. The energy required to transmit a bit is P/R . In the without-CSI model, a scheduled node will transmit only if it has energy qP/R . In the with-CSI model, a scheduled node will transmit only if it has energy $cT_f + qP/R$ and has a good channel.

As before, the absolute error with quantization is $\chi = |Y_{\text{max}} - \hat{Y}_{\text{meas}}|$, and the MAE is

$$\mathbb{E}[\chi] = \mathbb{E} \left[|Y_{\text{max}} - \hat{Y}_{\text{meas}}| \right] = \mathbb{E}[Y_{\text{max}} - \hat{Y}_{\text{meas}}], \quad (11)$$

where the last equality holds because $\hat{Y}_i \leq Y_i$. Hence, determining the inf of the MAE is equivalent to:

$$\begin{aligned} & \sup_{P,K,q} \mathbb{E}[\hat{Y}_{\text{meas}}] \\ & \text{s.t. } P \geq 0, \\ & 1 \leq K \leq N, \\ & 1 \leq q \leq \lfloor RT_s \rfloor. \end{aligned} \quad (12)$$

Let $\bar{\chi}_{K,q}^*$ denote the infimum MAE for a given K and q . First, we derive $\bar{\chi}_{K,q}^*$ in closed form. In Section V, we numerically optimize it over K and q .

Theorem 3: In the without-CSI model with quantization $\bar{\chi}_{K,q}^* = \mathbb{E}[Y_{N:N}] - \hat{Y}_1$, where

$$\hat{Y}_1 = \begin{cases} \frac{\bar{H}T_s R}{K\xi q e} \sum_{l=1}^K \left(1 - \frac{\bar{H}T_s R}{K\xi q e}\right)^{K-l} \sum_{j=1}^{2q} v_{j-1} (F_{Y_{l:K}}(v_j) - F_{Y_{l:K}}(v_{j-1})), & 0 < \bar{H} < \frac{K\xi q}{T_s R}, \\ e^{-\frac{K\xi q}{\bar{H}T_s R}} \sum_{l=1}^K \left(1 - e^{-\frac{K\xi q}{\bar{H}T_s R}}\right)^{K-l} \sum_{j=1}^{2q} v_{j-1} (F_{Y_{l:K}}(v_j) - F_{Y_{l:K}}(v_{j-1})), & \bar{H} \geq \frac{K\xi q}{T_s R}. \end{cases} \quad (13a)$$

$$\hat{Y}_1 = \begin{cases} \frac{\bar{H}T_s R}{K\xi q e} \sum_{l=1}^K \left(1 - \frac{\bar{H}T_s R}{K\xi q e}\right)^{K-l} \sum_{j=1}^{2q} v_{j-1} (F_{Y_{l:K}}(v_j) - F_{Y_{l:K}}(v_{j-1})), & 0 < \bar{H} < \frac{K\xi q}{T_s R}, \\ e^{-\frac{K\xi q}{\bar{H}T_s R}} \sum_{l=1}^K \left(1 - e^{-\frac{K\xi q}{\bar{H}T_s R}}\right)^{K-l} \sum_{j=1}^{2q} v_{j-1} (F_{Y_{l:K}}(v_j) - F_{Y_{l:K}}(v_{j-1})), & \bar{H} \geq \frac{K\xi q}{T_s R}. \end{cases} \quad (13b)$$

The optimal transmission power $P_{K,q}^*$ is given by

$$P_{K,q}^* = \begin{cases} \frac{N\xi}{T_s}, & 0 < \bar{H} < \frac{K\xi q}{T_s R}, \\ \frac{N\bar{H}R}{Kq}, & \bar{H} \geq \frac{K\xi q}{T_s R}. \end{cases} \quad (14a)$$

$$P_{K,q}^* = \begin{cases} \frac{N\xi}{T_s}, & 0 < \bar{H} < \frac{K\xi q}{T_s R}, \\ \frac{N\bar{H}R}{Kq}, & \bar{H} \geq \frac{K\xi q}{T_s R}. \end{cases} \quad (14b)$$

Proof: The proof is relegated to Appendix C. ■

As before, for the unquantized case, we see that when the node is energy-starved (cf. (14a)), $P_{K,q}^*$ is a constant. Once \bar{H} exceeds a threshold, the optimal power increases with it (cf. (14b)). In this regime, as q increases, $P_{K,q}^*$ decreases as a node transmits for a longer duration. In contrast to the unquantized scenario, an additional factor that appears now is the number of quantization bits q . It affects the threshold, which delineates the energy-starved regime, and $P_{K,q}^*$.

Theorem 4: Define $\Omega'_1 = W_0 \left(\frac{KN\xi q}{T_s R(N\bar{H} - KcT_f)} \right)$ and $\Omega'_2 = W_0 \left(\frac{1}{2} \sqrt{\frac{N\xi q}{T_s R c T_f}} \right)$. In the with-CSI model with quantization, $\bar{\chi}_{K,q}^* = \mathbb{E}[Y_{N:N}] - \hat{Y}_2$, where

$$\hat{Y}_2 = \begin{cases} \sigma'_1 \sum_{l=1}^K (1 - \sigma'_1)^{K-l} \sum_{j=1}^{2q} v_{j-1} (F_{Y_{l:K}}(v_j) - F_{Y_{l:K}}(v_{j-1})), & \bar{H} \geq \frac{KcT_f}{N}, \Omega'_1 \leq 2\Omega'_2, \\ \sigma'_2 \sum_{l=1}^K (1 - \sigma'_2)^{K-l} \sum_{j=1}^{2q} v_{j-1} (F_{Y_{l:K}}(v_j) - F_{Y_{l:K}}(v_{j-1})), & \text{otherwise,} \end{cases} \quad (15a)$$

$$\hat{Y}_2 = \begin{cases} \sigma'_1 \sum_{l=1}^K (1 - \sigma'_1)^{K-l} \sum_{j=1}^{2q} v_{j-1} (F_{Y_{l:K}}(v_j) - F_{Y_{l:K}}(v_{j-1})), & \bar{H} \geq \frac{KcT_f}{N}, \Omega'_1 \leq 2\Omega'_2, \\ \sigma'_2 \sum_{l=1}^K (1 - \sigma'_2)^{K-l} \sum_{j=1}^{2q} v_{j-1} (F_{Y_{l:K}}(v_j) - F_{Y_{l:K}}(v_{j-1})), & \text{otherwise,} \end{cases} \quad (15b)$$

$\sigma'_1 = \frac{\Omega'_1 T_s R(N\bar{H} - KcT_f)}{KN\xi q}$, and $\sigma'_2 = \frac{4T_s R\bar{H}\Omega'_2}{K\xi q + 2K\xi q\Omega'_2}$. The optimal transmit power $P_{K,q}^*$ that achieves it is given by

$$P_{K,q}^* = \begin{cases} \frac{N\xi}{T_s \Omega'_1}, & \bar{H} \geq \frac{KcT_f}{N}, \Omega'_1 \leq 2\Omega'_2, \\ \frac{N\xi}{2T_s \Omega'_1}, & \text{otherwise.} \end{cases} \quad (16a)$$

$$P_{K,q}^* = \begin{cases} \frac{N\xi}{T_s \Omega'_1}, & \bar{H} \geq \frac{KcT_f}{N}, \Omega'_1 \leq 2\Omega'_2, \\ \frac{N\xi}{2T_s \Omega'_1}, & \text{otherwise.} \end{cases} \quad (16b)$$

Proof: The proof is relegated to Appendix D. ■

Compared to Theorems 1 and 2, we see that the number of bits q affects both constants Ω'_1 and Ω'_2 , and, thus, affects \hat{Y}_1 , \hat{Y}_2 , and the optimal transmit power. Again, the optimal transmit power is a constant in the energy-starved regime and increases with \bar{H} in the energy rich regime.

V. NUMERICAL RESULTS

We now present Monte Carlo simulations that average over a duration of 10^5 DCRs, and compare them with our analytical results. For the purpose of illustration, we set $\omega = 8$ dB, $\alpha = 0.1$, $T_f = T_s = 88 \mu\text{s}$, $W = 257.6$ kHz, $\eta = 10$ dB, and $\Delta = 300$ K.¹ The nodes are at a distance of 101.3 m from the FN, the carrier frequency is 2.4 GHz, and the path-loss exponent is 4. We use the simplified path-loss model with a 10 m reference distance [22, Chapter 2]. This choice of parameters ensures that $\gamma_0/(\eta k_B \Delta W T_s)$ is equal to a round figure of 10^8 , where γ_0 turns out to be 9.393×10^{-11} . The Bernoulli EH model is simulated [29]. In every DCR, 50 nJ of energy is harvested with a probability ρ . Note that other path-loss models or DCR durations can be easily analyzed. Our goal is to capture the combined effect of various system parameters in determining how the EH WSN behaves.²

In the figures that follow, instead of \bar{H} , we use the insightful dimension-free normalized ratio $\bar{H}\gamma_0/(\eta k_B \Delta W T_s)$, which is the average SNR if the node transmits with power \bar{H}/T_s . Similarly, instead of cT_f , we use the dimension-free ratio $cT_f\gamma_0/(\eta k_B \Delta W T_s)$.

A. Results for Unquantized Measurements

Fig. 2 plots the normalized optimal transmit power $P_K^* \gamma_0/(\eta k_B \Delta W)$ as a function of the normalized average harvested energy $\bar{H}\gamma_0/(\eta k_B \Delta W T_s)$. Results for the without-CSI and with-CSI models are shown and compared. For the latter model, results for three different $cT_f\gamma_0/(\eta k_B \Delta W T_s)$, which captures the energy cost of acquiring CSI, are shown. For benchmarking purposes, the results for the ideal scenario in which the cost of acquiring CSI is zero are also shown.

Consider, first, the without-CSI model. Here, when $\bar{H} < K\xi = 3$ dB, a node is energy-starved and transmits with a constant energy so that the SNR is fixed at ω (cf. Theorem 1). For $\bar{H} \geq 3$ dB, the transmit energy becomes proportional to \bar{H} to improve the probability that the transmitted packet gets decoded by the FN. For the with-CSI model, when $c = 0$, P_K^* strictly increases as \bar{H} increases. On the other hand, the trends are different for $c > 0$. Now, as the node expends energy to

¹These values of ω and α correspond to a rate $R = 0.71$ bits/s/Hz in the quantized measurement model.

²As mentioned, an alternate paradigm for computing the maximum is block computation [2], [3]. In it, the nodes buffer the measurements taken over several time instants, and then compute the maximum for each of these time instants in one go. We do not compare with it because the corresponding results for it for an EH WSN are not available. Further, block computation will outperform one-shot computation because the nodes in the former can buffer data and process the blocks of buffered data. However, this comes at the expense of an impractically large delay, which increases with the block size [2].

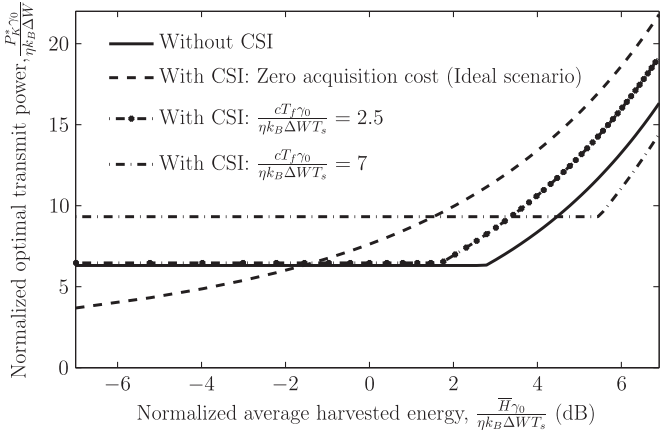


Fig. 2. Normalized optimal transmit power $\frac{P_K^*\gamma_0}{\eta k_B \Delta W T_s}$ as a function of normalized average harvested energy $\frac{\bar{H}\gamma_0}{\eta k_B \Delta W T_s}$ ($N = 10$, $K = 3$, and exponentially distributed independent readings with unit mean). Lines indicate the optimal values obtained from Theorems 1 and 2.

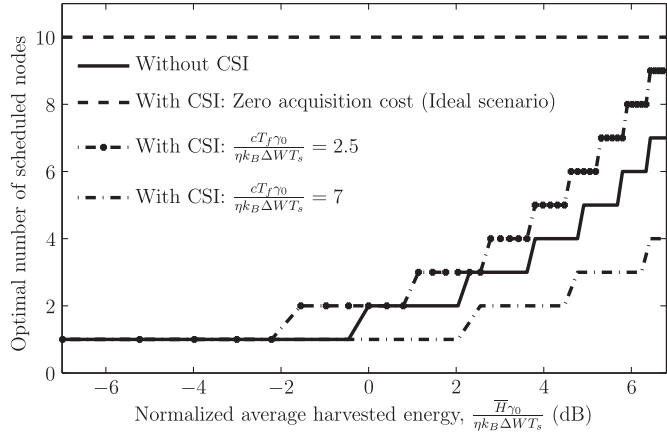


Fig. 3. Optimal number of scheduled nodes as a function of normalized average harvested energy $\frac{\bar{H}\gamma_0}{\eta k_B \Delta W T_s}$ ($N = 10$ and exponentially distributed independent readings with unit mean). Lines indicate the optimal values obtained by numerically optimizing $\bar{\chi}_K^*$, which is given by Theorems 1 and 2.

acquire CSI, P_K^* is set such that the SNR is at least $\omega/(2\Omega_2)$ (cf. Theorem 2) to ensure at least a minimum packet decoding probability. At low \bar{H} , P_K^* is a constant, and it increases for higher \bar{H} (cf. (8)). When the cost of acquiring CSI is high, the node has relatively less energy to transmit compared to the without-CSI model. Hence, in the energy-starved regime, the node transmits less often, but with a higher power to improve the odds that its reading is decoded by the FN.

Fig. 3 plots the optimal number of nodes K^* as a function of $\bar{H}\gamma_0/(\eta k_B \Delta W T_s)$ for both CSI models. For the with-CSI model with zero acquisition cost, having all the nodes transmit turns out to be always optimal. This is because a node consumes energy only when it transmits, which happens only when its channel fade is good. It is the optimal transmit power that now changes with \bar{H} , as we saw in Fig. 2. The trends are different in the without-CSI model and the with-CSI model for $c > 0$. When the EH nodes are energy-starved, fewer nodes are scheduled as this saves energy for future transmissions. As \bar{H}

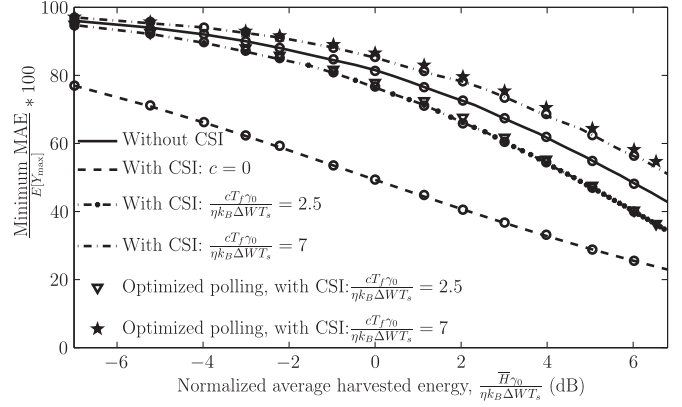


Fig. 4. Minimum MAE as a function of normalized average harvested energy $\frac{\bar{H}\gamma_0}{\eta k_B \Delta W T_s}$ ($N = 10$ and exponentially distributed independent readings with unit mean). Lines plot the optimal values obtained by numerically optimizing $\bar{\chi}_K^*$, which is given in Theorems 1 and 2. Simulation results are indicated by the marker ‘o’.

increases, K^* increases so as to improve the measurement accuracy. As the CSI acquisition cost increases, scheduling fewer nodes is better as it conserves energy for future transmissions.

Fig. 4 plots the minimum MAE as a function of $\bar{H}\gamma_0/(\eta k_B \Delta W T_s)$. The error range for the simulation results is $\pm 0.5\%$ for a confidence interval of 99.8%. We find that as \bar{H} increases, the minimum MAE decreases because the optimal transmit power increases. While CSI helps reduce transmit energy by avoiding transmissions when the channel is in a deep fade, the cost of acquiring it offsets its benefits. Hence, the minimum MAE is the lowest for the with-CSI model with $c = 0$ and increases as c increases. In both these cases, the with-CSI model outperforms the without-CSI model. However, for a high acquisition cost of $cT_f\gamma_0/(\eta k_B \Delta W T_s) = 7$, the minimum MAE with CSI exceeds that without CSI.

Also shown for comparison is the MAE in which all the nodes transmit ($K = N$), with the optimal transmit power being determined from Theorem 2. Its MAE is more than the optimal MAE by 1 to 2% for $c > 0$.

B. Results for Quantized Measurements

Fig. 5 plots the minimum MAE as a function of $\bar{H}\gamma_0/(\eta k_B \Delta W T_s)$ with quantized measurements obtained by numerically optimizing the MAE expressions in Theorems 3 and 4 with respect to the number of scheduled nodes K and number of quantized bits q . As \bar{H} increases, the MAE again decreases. The MAEs in the with-CSI model with $c = 0$ and $cT_f\gamma_0/(\eta k_B \Delta W T_s) = 7$ are respectively lower and higher than in the without-CSI model. This is due to reasons explained earlier. Table I lists the corresponding optimal numbers of scheduled nodes and bits. As \bar{H} increases, the optimal number of scheduled nodes and quantization bits both increase. The only exception is the with-CSI model, with $c = 0$. Here, it is optimal to schedule all the nodes all the time as the nodes are energy-rich. We find that the optimal number of scheduled nodes in the without-CSI model and the with-CSI model with $c = 0$ is greater than that for the with-CSI model with

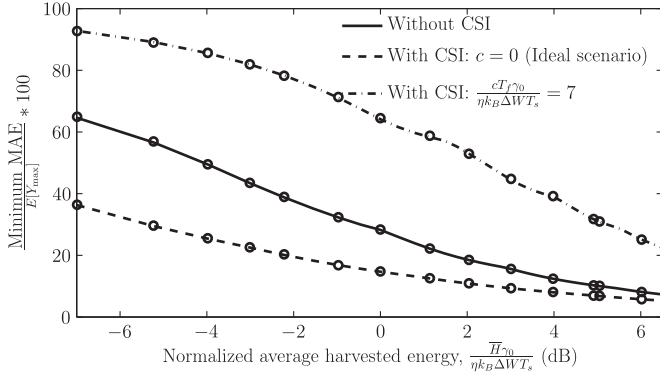


Fig. 5. Minimum MAE as a function of normalized average harvested energy $\frac{\bar{H}\gamma_0}{\eta k_B \Delta W T_s}$ ($N = 10$ and uniformly distributed independent readings over $[0,1]$). Lines plot the optimal values obtained by numerically optimizing $\bar{\chi}_{K,q}^*$, which is given in Theorems 3 and 4. Simulation results are indicated by the marker 'o'.

TABLE I
OPTIMAL NUMBER OF SCHEDULED NODES AND TRANSMITTED BITS
($N = 10$ AND UNIFORMLY DISTRIBUTED INDEPENDENT
READINGS OVER $[0,1]$)

$\frac{\bar{H}\gamma_0}{\eta k_B \Delta W T_s}$ (dB)	(Scheduled nodes, Transmitted bits)		
	Without-CSI model	With-CSI model	
		$\frac{cT_f\gamma_0}{\eta k_B \Delta W T_s} = 0$ (Ideal scenario)	$\frac{cT_f\gamma_0}{\eta k_B \Delta W T_s} = 7$
-10	(2, 1)	(10, 2)	(1, 3)
-7	(5, 1)	(10, 3)	(1, 3)
-3	(6, 2)	(10, 4)	(1, 3)
0	(10, 2)	(10, 4)	(1, 3)
3	(10, 4)	(10, 5)	(2, 4)
6	(10, 5)	(10, 6)	(4, 4)

$cT_f\gamma_0/(\eta k_B \Delta W T_s) = 7$. This is because as the scheduled nodes expend a considerable amount of energy acquiring CSI, fewer nodes get scheduled to conserve the energy that remains.

With finite energy buffers, extensive simulations show that for the same \bar{H} , the optimal number of scheduled nodes increases as the energy buffer capacity decreases to reduce the odds of energy wastage due to buffer overflow. When the number of scheduled nodes is the same, the optimal number of bits is a non-decreasing function of the buffer capacity.

VI. CONCLUSIONS

We analyzed the mean absolute error of an EH WSN in estimating the maximum sensor reading, for any stationary and ergodic EH processes and for any stationary and ergodic sensor reading process in which the readings have a continuous probability distribution with positive support. Our results hold for any DCR duration so long as the slot duration is less than the channel coherence time of the sensor readings.³ We saw that for the objective function studied, the optimal number of scheduled

³In the with-CSI model, the DCR duration needs to be less than the channel coherence time of the EH nodes so that the CSI acquired at the beginning of the DCR remains relevant for the entire DCR.

nodes and bits, and the optimal transmit power depend on the total number of nodes in the WSN, means of EH and channel fading processes, availability of CSI, and the cost of acquiring it. The optimal values of transmit power, number of scheduled nodes, and quantization bits increased with the average EH rate. Also, the with-CSI model with high acquisition costs performed worse than the without-CSI model.

Several interesting avenues for research exist. These include incorporating frequency-selective channels and associated transmitter/receiver architectures, studying MAC protocols, and investigating general network function computation problems in EH WSNs.

APPENDIX

A. Proof of Theorem 1

Since $Y_{\max} \geq Y_{\text{meas}}$, evaluating $\bar{\chi}_{K,q}^*$ is equivalent to determining $\sup \mathbb{E}[Y_{\text{meas}}]$. The SNR at the FN exceeds ω if the channel power gain of a scheduled node exceeds $\omega \eta k_B \Delta W / P$. Let ψ be the probability of this event. For Rayleigh fading,

$$\psi = \Pr \left(h_i \geq \frac{\omega \eta k_B \Delta W}{P} \right) = e^{-\frac{\omega \eta k_B \Delta W}{\gamma_0 P}} = e^{-\frac{N\xi}{PT_s}}. \quad (17)$$

Let ζ be the probability of the event that a node's energy buffer has the required energy for transmission. As the channel fading process of a node is i.i.d. across time, the above two events are mutually independent. Hence, a scheduled node's reading is received successfully by the FN with probability $\zeta\psi$.

In a DCR, let \mathcal{M}_l^K denote the event that given that K nodes are scheduled for transmission, only the l^{th} smallest reading among them is decoded by the FN and the $(l+1)^{\text{th}}, (l+2)^{\text{th}}, \dots, K^{\text{th}}$ smallest readings are not decoded. As the transmission schedule, the EH processes, and the channel fading processes of the nodes are independent, $\Pr(\mathcal{M}_l^K) = \zeta\psi(1 - \zeta\psi)^{K-l}$, for $1 \leq l \leq K$. From the law of total probability, the expected maximum reading at the FN is

$$\begin{aligned} \mathbb{E}[Y_{\text{meas}}] &= \sum_{l=1}^K \mathbb{E}[Y_{\text{meas}} | \mathcal{M}_l^K] \Pr(\mathcal{M}_l^K), \\ &= \sum_{l=1}^K \mathbb{E}[Y_{l:K}] \zeta\psi(1 - \zeta\psi)^{K-l}. \end{aligned} \quad (18)$$

Let \bar{U} denote the average energy consumed by a node in a DCR. From the law of conservation of energy, it follows that

$$\bar{U} \leq \bar{H}. \quad (19)$$

A node is scheduled in a DCR with probability K/N , and it transmits with energy PT_s with probability ζ . Hence, the average energy \bar{U} used by a node to transmit a reading is

$$\bar{U} = \frac{K}{N} \zeta PT_s. \quad (20)$$

Using the above, we now evaluate $\sup \mathbb{E}[Y_{\text{meas}}]$ in the following three regimes: $0 \leq P < N\bar{H}/(KT_s)$, $P = N\bar{H}/(KT_s)$,

and $N\bar{H}/(KT_s) < P < \infty$. As we shall see below, ζ changes from 1 in the first two regimes to strictly less than 1 in the last regime. We shall refer to $\zeta < 1$ as the *energy constrained* regime and $\zeta = 1$ as the *energy unconstrained* regime.

1) When $0 \leq P < N\bar{H}/(KT_s)$: In this regime, it can be shown that in steady state, $\bar{H} > \bar{U}$. Thus, the energy of the EH node becomes infinite. Hence, $\zeta = 1$, and (18) reduces to

$$\mathbb{E}[Y_{\text{meas}}] = \sum_{l=1}^K \mathbb{E}[Y_{l:K}] \psi (1 - \psi)^{K-l}, \quad (21)$$

$$\begin{aligned} &= \sum_{l=1}^{K-1} (\mathbb{E}[Y_{l:K}] - \mathbb{E}[Y_{l+1:K}]) (1 - \psi)^{K-l} \\ &\quad - \mathbb{E}[Y_{1:K}] (1 - \psi)^K + \mathbb{E}[Y_{K:K}]. \end{aligned} \quad (22)$$

Differentiating $\mathbb{E}[Y_{\text{meas}}]$ with respect to ψ , we get

$$\begin{aligned} \frac{d}{d\psi} \mathbb{E}[Y_{\text{meas}}] &= \sum_{l=1}^{K-1} (K-l) (\mathbb{E}[Y_{l+1:K}] - \mathbb{E}[Y_{l:K}]) \\ &\quad \times (1 - \psi)^{K-l-1} + K \mathbb{E}[Y_{1:K}] (1 - \psi)^{K-1}. \end{aligned} \quad (23)$$

As $\mathbb{E}[Y_{l+1:K}] \geq \mathbb{E}[Y_{l:K}]$, $\mathbb{E}[Y_{1:K}] > 0$, and $\psi < 1$, we find that $\frac{d}{d\psi} \mathbb{E}[Y_{\text{meas}}] > 0$. Hence, $\mathbb{E}[Y_{\text{meas}}]$ is monotonically increasing in ψ . Since $P \in [0, N\bar{H}/(KT_s))$, from (17) we get $\psi \in [0, e^{-\frac{K\xi}{\bar{H}}})$. Therefore, from (21), we get

$$\sup_{0 \leq P < \frac{N\bar{H}}{KT_s}} \mathbb{E}[Y_{\text{meas}}] = e^{-\frac{K\xi}{\bar{H}}} \sum_{l=1}^K \mathbb{E}[Y_{l:K}] \left(1 - e^{-\frac{K\xi}{\bar{H}}}\right)^{K-l}, \quad (24)$$

and is achieved as $P \rightarrow \left(\frac{N\bar{H}}{KT_s}\right)^-$.

2) When $P = N\bar{H}/(KT_s)$: Here, $\bar{U} = \bar{H}\zeta$. It can be shown that $\zeta = 1$.⁴ From (17), $\psi = e^{-\frac{K\xi}{\bar{H}}}$. Substituting this in (21) yields

$$\mathbb{E}[Y_{\text{meas}}] = e^{-\frac{K\xi}{\bar{H}}} \sum_{l=1}^K \mathbb{E}[Y_{l:K}] \left(1 - e^{-\frac{K\xi}{\bar{H}}}\right)^{K-l}. \quad (25)$$

3) When $N\bar{H}/(KT_s) < P < \infty$: Here, using (20), we get

$$\bar{U} > \bar{H}\zeta. \quad (26)$$

This implies that $0 \leq \zeta < 1$, which also implies that $\bar{U} = \bar{H}$.⁵ From (20), we then get

$$\zeta = \frac{N\bar{H}}{KPT_s}. \quad (27)$$

⁴We prove this by contradiction. If $\zeta < 1$, then $\bar{U} < \bar{H}$. Hence, the node's energy increases to ∞ , which implies that $\zeta = 1$, which is a contradiction.

⁵This can be proved by contradiction. If $\zeta = 1$, using (26), we get $\bar{U} > \bar{H}$, which contradicts (19).

Rewriting (18), we get

$$\begin{aligned} \mathbb{E}[Y_{\text{meas}}] &= \sum_{l=1}^{K-1} (\mathbb{E}[Y_{l:K}] - \mathbb{E}[Y_{l+1:K}]) (1 - \zeta\psi)^{K-l} \\ &\quad - \mathbb{E}[Y_{1:K}] (1 - \zeta\psi)^K + \mathbb{E}[Y_{K:K}]. \end{aligned}$$

Similar to (23), it can be shown that $\mathbb{E}[Y_{\text{meas}}]$ is a monotonically increasing function of $\zeta\psi$. Thus, the optimal power that maximizes $\zeta\psi$ is the same as the one that maximizes $\mathbb{E}[Y_{\text{meas}}]$. We determine it below. From (17) and (27), we have

$$\zeta\psi = \frac{N\bar{H}}{KPT_s} e^{-\frac{N\xi}{PT_s}}. \quad (28)$$

Differentiating $\zeta\psi$ with respect to P , we get $\frac{d}{dP} \zeta\psi = \frac{N\bar{H}}{KT_s P^2} e^{-\frac{N\xi}{PT_s}} \left(\frac{N\xi}{PT_s} - 1\right)$. If $\bar{H} < K\xi$, it follows that $\frac{d}{dP} \zeta\psi > 0$ when $P \in (N\bar{H}/(KT_s), N\xi/T_s)$. Further, $\frac{d}{dP} \zeta\psi = 0$ when $P = N\xi/T_s$, and $\frac{d}{dP} \zeta\psi < 0$ when $P > N\xi/T_s$. Hence, $\zeta\psi$ achieves its maximum at $P = N\xi/T_s$ when $\bar{H} < K\xi$. On the other hand, if $\bar{H} \geq K\xi$, then $N\xi/T_s \leq N\bar{H}/(KT_s) < P$. Therefore, $\frac{d}{dP} \zeta\psi < 0$. Thus, $\zeta\psi$ reaches its supremum (sup) as $P \rightarrow \left(\frac{N\bar{H}}{KT_s}\right)^+$. Substituting these values of P in (18) and (28), when $0 < \bar{H} < K\xi$, yields

$$\sup_{\frac{N\bar{H}}{KT_s} < P < \infty} \mathbb{E}[Y_{\text{meas}}] = \frac{\bar{H}}{K\xi e} \sum_{l=1}^K \mathbb{E}[Y_{l:K}] \left(1 - \frac{\bar{H}}{K\xi e}\right)^{K-l}, \quad (29a)$$

and when $\bar{H} \geq K\xi$, we get

$$\sup_{\frac{N\bar{H}}{KT_s} < P < \infty} \mathbb{E}[Y_{\text{meas}}] = e^{-\frac{K\xi}{\bar{H}}} \sum_{l=1}^K \mathbb{E}[Y_{l:K}] \left(1 - e^{-\frac{K\xi}{\bar{H}}}\right)^{K-l}. \quad (29b)$$

The expression for $\sup \mathbb{E}[Y_{\text{meas}}]$ is the same in (24), (29b), and (25). The only exception is (29a), which occurs for $\bar{H} < K\xi$. Thus, when $\bar{H} \geq K\xi$, $\sup_{P \geq 0} \mathbb{E}[Y_{\text{meas}}]$ is given by (25) and the optimal transmission energy is $P_K^* = N\bar{H}/(KT_s)$.

When $\bar{H} < K\xi$, for $N\bar{H}/(KT_s) < P < \infty$, we know that the solution in (29a) is optimal, and not that in (29b). Therefore,

$$\begin{aligned} \sup_{\frac{N\bar{H}}{KT_s} < P < \infty} \mathbb{E}[Y_{\text{meas}}] &> e^{-\frac{K\xi}{\bar{H}}} \sum_{l=1}^K \mathbb{E}[Y_{l:K}] \left(1 - e^{-\frac{K\xi}{\bar{H}}}\right)^{K-l}, \\ &= \sup_{0 < P \leq \frac{N\bar{H}}{KT_s}} \mathbb{E}[Y_{\text{meas}}], \end{aligned} \quad (30)$$

where the last equality follows from (24) and (25). Thus, in this regime, $P_K^* = N\xi/T_s$ and $\sup_{P \geq 0} \mathbb{E}[Y_{\text{meas}}]$ is given by (29a). Since the supremum is achievable, it also follows that the maximum of $\mathbb{E}[Y_{\text{meas}}]$ exists and $\bar{\chi}_K^*$ is the minimum MAE. Hence, the result follows.

B. Proof of Theorem 2

A node is scheduled in a DCR with probability K/N . In the with-CSI model, a scheduled EH node estimates its channel

gain only if it has enough energy for CSI acquisition and packet transmission, which is $cT_f + PT_s$. Let ζ be the probability of this event. A scheduled node transmits only if its channel power gain exceeds $\omega\eta k_B \Delta W/P$. As in Appendix A, let ψ be the probability of this event. It is given by (17). Thus, a scheduled node expends energy cT_f with probability $\zeta(1 - \psi)$, and it expends $cT_f + PT_s$ with probability $\zeta\psi$. Hence, the average energy consumed by a node is given by

$$\bar{U} = \frac{K}{N} \zeta (cT_f + PT_s \psi). \quad (31)$$

We consider the scenarios $\bar{H} < KcT_f/N$ and $\bar{H} \geq KcT_f/N$ separately below.

1) *When $\bar{H} < KcT_f/N$:* Here, $\zeta < 1$.⁶ Since an EH node when scheduled runs out of energy to transmit with a strictly positive probability, it follows from the law of conservation of energy that the average energy harvested equals the average energy consumed: $\bar{H} = \bar{U} = K\zeta(cT_f + PT_s\psi)/N$. Rearranging terms and substituting $\psi = e^{-\frac{N\xi}{PT_s}}$ (cf. (17)), yields

$$\zeta\psi = \frac{N\bar{H}}{K(cT_f + PT_s e^{-\frac{N\xi}{PT_s}})} e^{-\frac{N\xi}{PT_s}}. \quad (32)$$

Differentiating $\zeta\psi$ with respect to P , and simplifying yields

$$\frac{d}{dP} \zeta\psi = \frac{\frac{N\bar{H} e^{-\frac{N\xi}{PT_s}}}{K} \left(cT_f \frac{N\xi}{T_s P^2} - T_s e^{-\frac{N\xi}{PT_s}} \right)}{\left(cT_f + PT_s e^{-\frac{N\xi}{PT_s}} \right)^2}. \quad (33)$$

The above derivative is 0 when $P = N\xi/(2T_s\Omega_2)$, where $\Omega_2 = W_0\left(\frac{1}{2}\sqrt{\frac{N\xi}{cT_f}}\right)$. Also, it can be shown that $\frac{d}{dP} \zeta\psi > 0$ when $0 \leq P < N\xi/(2T_s\Omega_2)$, and $\frac{d}{dP} \zeta\psi < 0$ when $N\xi/(2T_s\Omega_2) < P < \infty$. Thus, $P_K^* = N\xi/(2T_s\Omega_2)$. Substituting this in (18) and (32) yields (7b).

2) *When $\bar{H} \geq KcT_f/N$:* Consider the following three regimes: i) $0 \leq P < N\xi/(T_s\Omega_1)$, ii) $P = N\xi/(T_s\Omega_1)$, and iii) $N\xi/(T_s\Omega_1) < P < \infty$, where $\Omega_1 = W_0\left(\frac{KN\xi}{N\bar{H} - KcT_f}\right)$. As we shall see, these demarcate the regimes where a node changes from being energy unconstrained to energy constrained.

i) *When $0 \leq P < N\xi/(T_s\Omega_1)$:* Substituting this inequality in (17) and (31) and using $\zeta \leq 1$ and (17) we get

$$\bar{U} \leq \frac{K}{N} \left(cT_f + PT_s e^{-\frac{N\xi}{PT_s}} \right) < \frac{K}{N} \left(cT_f + \frac{N\xi}{\Omega_1} e^{-\Omega_1} \right).$$

From the definition of Lambert W-function, we have $\Omega_1 e^{\Omega_1} = \frac{KN\xi}{N\bar{H} - KcT_f}$. Therefore, $\bar{U} < \frac{K}{N} \left(cT_f + \frac{N\xi}{\frac{KN\xi}{N\bar{H} - KcT_f}} \right) = \bar{H}$.

Since $\bar{U} < \bar{H}$, the energy in the node's energy buffer will tend to ∞ in steady state. Hence, $\zeta = 1$.

⁶We prove this by contradiction. If $\zeta = 1$, using (19) and (31), we would get $P < 0$, which is impossible.

Similar to Appendix A1, $\mathbb{E}[Y_{\text{meas}}]$ is monotonically increasing in ψ when $\zeta = 1$. Also, as $P \in [0, N\xi/(T_s\Omega_1))$, ψ in (17) lies in between 0 and $e^{-\Omega_1}$. Therefore, from (21),

$$\sup_{0 \leq P < \frac{N\xi}{T_s\Omega_1}} \mathbb{E}[Y_{\text{meas}}] = e^{-\Omega_1} \sum_{l=1}^K \mathbb{E}[Y_{l:K}] (1 - e^{-\Omega_1})^{K-l}, \quad (34)$$

which occurs as $P \rightarrow \left(\frac{N\xi}{T_s\Omega_1}\right)^-$.

ii) *When $P = N\xi/(T_s\Omega_1)$:* In this case, $\psi = e^{-\Omega_1}$ (cf. (17)) and $\zeta = 1$.⁷ Therefore, (18) reduces to

$$\mathbb{E}[Y_{\text{meas}}] = e^{-\Omega_1} \sum_{l=1}^K \mathbb{E}[Y_{l:K}] (1 - e^{-\Omega_1})^{K-l}. \quad (35)$$

Combining this with (34), we find that

$$\sup_{0 \leq P \leq \frac{N\xi}{T_s\Omega_1}} \mathbb{E}[Y_{\text{meas}}] = e^{-\Omega_1} \sum_{l=1}^K \mathbb{E}[Y_{l:K}] (1 - e^{-\Omega_1})^{K-l}. \quad (36)$$

iii) *When $N\xi/(T_s\Omega_1) < P < \infty$:* Substituting this inequality in (31), we get $\bar{U} > \frac{K}{N} \zeta \left(cT_f + \frac{N\xi}{\Omega_1} e^{-\Omega_1} \right)$. Using $W_0(x)e^{W_0(x)} = x$ to simplify the above inequality, and applying (19), we get $\bar{U} > \frac{K}{N} \zeta \left(cT_f + \frac{N\xi}{\frac{KN\xi}{N\bar{H} - KcT_f}} \right) = \bar{H} \zeta \geq \bar{U} \zeta$. Therefore, $\zeta < 1$. As proved in Appendix A3, for $\zeta < 1$, $\mathbb{E}[Y_{\text{meas}}]$ is monotonically increasing in $\zeta\psi$. Hence, the power that achieves the supremum of $\zeta\psi$ also achieves that of $\mathbb{E}[Y_{\text{meas}}]$.

From (33), we know that $\frac{d\zeta\psi}{dP} = 0$ at $P = N\xi/(2T_s\Omega_2)$. It can be shown that $\frac{d\zeta\psi}{dP} > 0$ for $N\xi/(T_s\Omega_1) < P < N\xi/(2T_s\Omega_2)$ and $\frac{d\zeta\psi}{dP} < 0$ for $P > N\xi/(2T_s\Omega_2)$. Now, $N\xi/(2T_s\Omega_2)$ is an interior point of $(N\xi/(T_s\Omega_1), \infty)$ when $\Omega_1 > 2\Omega_2$, and is an exterior point when $\Omega_1 \leq 2\Omega_2$. Hence, the supremum of $\zeta\psi$ is given as follows. In the former case, $\sup_{\frac{N\xi}{T_s\Omega_1} < P < \infty} \mathbb{E}[Y_{\text{meas}}]$ is achieved at $P = N\xi/(2T_s\Omega_2)$, and from (18) is given by

$$\sup_{\frac{N\xi}{T_s\Omega_1} < P < \infty} \mathbb{E}[Y_{\text{meas}}] = \sigma_2 \sum_{l=1}^K \mathbb{E}[Y_{l:k}] (1 - \sigma_2)^{K-l}, \quad (37)$$

where $\sigma_2 = \frac{4\bar{H}\Omega_2^2}{K\xi + 2K\xi\Omega_2}$.

In the latter case ($\Omega_1 \leq 2\Omega_2$), $N\xi/(T_s\Omega_1) \geq N\xi/(2T_s\Omega_2)$ and $\frac{d\zeta\psi}{dP} < 0$, for $P \in (N\xi/(T_s\Omega_1), \infty)$. Hence, $\sup_{\frac{N\xi}{T_s\Omega_1} < P < \infty} \mathbb{E}[Y_{\text{meas}}]$ is achieved as $P \rightarrow \left(\frac{N\xi}{T_s\Omega_1}\right)^+$. Substituting this in (32), it can be shown that $\zeta\psi \rightarrow e^{-\Omega_1}$. Applying these results to (18), we get

$$\sup_{\frac{N\xi}{T_s\Omega_1} < P < \infty} \mathbb{E}[Y_{\text{meas}}] = e^{-\Omega_1} \sum_{l=1}^K \mathbb{E}[Y_{l:K}] (1 - e^{-\Omega_1})^{K-l}. \quad (38)$$

⁷Using (31) and the fact $W_0(x)e^{W_0(x)} = x$ we get $\bar{U} = \zeta\bar{H}$. Let us assume that $\zeta < 1$, which implies $\bar{U} < \bar{H}$. Hence, a node's energy buffer tends to ∞ . This implies $\zeta = 1$, which is a contradiction. Hence, $\zeta = 1$.

Combining All Results for $\bar{H} \geq KcT_f/N$: Now, we combine all the above results to find $\sup_{0 \leq P < \infty} \mathbb{E}[Y_{\text{meas}}]$ for $\bar{H} \geq KcT_f/N$. Since $\sup \mathbb{E}[Y_{\text{meas}}]$ is different for $\Omega_1 > 2\Omega_2$ and $\Omega_1 \leq 2\Omega_2$, we treat them separately below.

a) *If $\Omega_1 > 2\Omega_2$:* From the discussion preceding (37), we know that for $P \in (N\xi/(T_s\Omega_1), \infty)$ the optimal power is $N\xi/(2T_s\Omega_2)$ and not $N\xi/(T_s\Omega_1)$. Therefore, if $P = N\xi/(T_s\Omega_1)$ is used, the corresponding expression of $\mathbb{E}[Y_{\text{meas}}]$ in (35) would be less than $\sup_{\frac{N\xi}{T_s\Omega_1} < P < \infty} \mathbb{E}[Y_{\text{meas}}]$. Hence, from (35),

$$\begin{aligned} \sup_{\frac{N\xi}{T_s\Omega_1} < P < \infty} \mathbb{E}[Y_{\text{meas}}] &> e^{-\Omega_1} \sum_{l=1}^K \mathbb{E}[Y_{l:K}] (1 - e^{-\Omega_1})^{K-l}, \\ &= \sup_{0 \leq P \leq \frac{N\xi}{T_s\Omega_1}} \mathbb{E}[Y_{\text{meas}}], \end{aligned} \quad (39)$$

where the last equality follows from (36). Hence, (39) implies that $\sup_{0 \leq P < \infty} \mathbb{E}[Y_{\text{meas}}] = \sup_{\frac{N\xi}{T_s\Omega_1} < P < \infty} \mathbb{E}[Y_{\text{meas}}]$, and is given by (7b). Further, the supremum is achieved at $P_K^* = N\xi/(2T_s\Omega_2)$, and, hence, is the maximum.

b) *If $\Omega_1 \leq 2\Omega_2$:* Since the expressions for the supremum of $\mathbb{E}[Y_{\text{meas}}]$ over $0 < P \leq N\xi/(T_s\Omega_1)$ in (36) and that over $N\xi/(T_s\Omega_1) < P < \infty$ in (38) are the same, it follows that they both are also the expression for the supremum over $0 \leq P < \infty$. Since it is achieved at $P_K^* = N\xi/(T_s\Omega_1)$, it is the maximum and (7a) follows.

C. Proof of Theorem 3

We first derive an expression for $\mathbb{E}[\hat{Y}_{\text{meas}}]$.

Expression for $\mathbb{E}[\hat{Y}_{\text{meas}}]$: When \mathcal{M}_l^K occurs, as the readings reported are quantized, we have $\hat{Y}_{\text{meas}} = \hat{Y}_{l:K}$. Using the law of total probability, as in Appendix A, we get

$$\mathbb{E}[\hat{Y}_{\text{meas}}] = \sum_{l=1}^K \mathbb{E}[\hat{Y}_{l:K}] \zeta \psi (1 - \zeta \psi)^{K-l}, \quad (40)$$

where ζ is the probability that a node has energy for transmission. In terms of the quantizer, $\mathbb{E}[\hat{Y}_{l:K}]$ can be written as

$$\begin{aligned} \mathbb{E}[\hat{Y}_{l:K}] &= \sum_{j=1}^{2^q} v_{j-1} \int_{v_{j-1}}^{v_j} f_{Y_{l:K}}(u) du, \\ &= \sum_{j=1}^{2^q} v_{j-1} (F_{Y_{l:K}}(v_j) - F_{Y_{l:K}}(v_{j-1})). \end{aligned} \quad (41)$$

Substituting the above equation in (40), we get

$$\begin{aligned} \mathbb{E}[\hat{Y}_{\text{meas}}] &= \sum_{l=1}^K \zeta \psi (1 - \zeta \psi)^{K-l} \\ &\quad \times \sum_{j=1}^{2^q} v_{j-1} (F_{Y_{l:K}}(v_j) - F_{Y_{l:K}}(v_{j-1})). \end{aligned} \quad (42)$$

Since a node is scheduled in a DCR with probability K/N , and it transmits q bits with energy qP/R and with probability ζ , the average transmit energy of a node is equal to

$$\bar{U} = \frac{K}{N} \zeta \frac{qP}{R}. \quad (43)$$

Determining the Supremum of $\mathbb{E}[\hat{Y}_{\text{meas}}]$: We first calculate the supremum of $\mathbb{E}[\hat{Y}_{\text{meas}}]$ in each of the following regimes: $0 \leq P < N\bar{H}R/(Kq)$, $P = N\bar{H}R/(Kq)$, and $N\bar{H}R/(Kq) < P < \infty$. As we shall see, the system changes from being energy unconstrained to energy constrained across these regimes.

1) *When $0 \leq P < N\bar{H}R/(Kq)$:* It can be shown that, in steady state, the energy of the EH node becomes infinite. Hence, $\zeta = 1$, and (42) reduces to

$$\begin{aligned} \mathbb{E}[\hat{Y}_{\text{meas}}] &= \sum_{l=1}^K \psi (1 - \psi)^{K-l} \\ &\quad \times \sum_{j=1}^{2^q} v_{j-1} (F_{Y_{l:K}}(v_j) - F_{Y_{l:K}}(v_{j-1})). \end{aligned} \quad (44)$$

Along lines similar to Appendix A1, it can be shown that $\mathbb{E}[\hat{Y}_{\text{meas}}]$ is monotonically increasing in ψ . As $P \in [0, N\bar{H}R/(Kq))$, from (17), ψ lies in the interval $\left[0, e^{-\frac{K\xi q}{\bar{H}RT_s}}\right)$. Therefore,

$$\begin{aligned} \sup_{0 \leq P < \frac{N\bar{H}R}{Kq}} \mathbb{E}[\hat{Y}_{\text{meas}}] &= e^{-\frac{K\xi q}{\bar{H}RT_s}} \sum_{l=1}^K \left(\left(1 - e^{-\frac{K\xi q}{\bar{H}RT_s}}\right)^{K-l} \right. \\ &\quad \left. \times \sum_{j=1}^{2^q} v_{j-1} (F_{Y_{l:K}}(v_j) - F_{Y_{l:K}}(v_{j-1})) \right), \end{aligned} \quad (45)$$

and occurs as $P \rightarrow \left(\frac{N\bar{H}R}{Kq}\right)^-$.

2) *When $P = N\bar{H}R/(Kq)$:* Using steps similar to Appendix A2, it can be shown that $\zeta = 1$. Here, $\psi = e^{-\frac{K\xi q}{\bar{H}RT_s}}$ (cf. (17)). Substituting these values for ζ and ψ in (44), we get

$$\begin{aligned} \mathbb{E}[\hat{Y}_{\text{meas}}] &= e^{-\frac{K\xi q}{\bar{H}RT_s}} \sum_{l=1}^K \left(1 - e^{-\frac{K\xi q}{\bar{H}RT_s}}\right)^{K-l} \\ &\quad \times \sum_{j=1}^{2^q} v_{j-1} (F_{Y_{l:K}}(v_j) - F_{Y_{l:K}}(v_{j-1})). \end{aligned} \quad (46)$$

3) *When $N\bar{H}R/(Kq) < P < \infty$:* Along lines similar to Appendix A3, it can be shown that in this regime, $\zeta < 1$ and $\bar{H} = \bar{U}$. From (43), we then get $\zeta = N\bar{H}R/(KqP)$. Again, using steps similar to those in Appendix A3, it can be shown that $\mathbb{E}[\hat{Y}_{\text{meas}}]$ is a monotonically increasing function of $\zeta \psi$, which achieves its supremum at $P = N\xi/T_s$ if $\bar{H} < K\xi q/(RT_s)$, and as $P \rightarrow \left(\frac{N\bar{H}R}{Kq}\right)^+$ if $\bar{H} \geq K\xi q/(RT_s)$.

Substituting these in (42), for $\bar{H} < K\xi q/(RT_s)$, we find $\sup_{\frac{N\bar{H}R}{Kq} < P < \infty} \mathbb{E}[\hat{Y}_{\text{meas}}]$

$$= \frac{\bar{H}T_s R}{K\xi q e} \sum_{l=1}^K \left(1 - \frac{\bar{H}T_s R}{K\xi q e}\right)^{K-l} \sum_{j=1}^{2^q} v_{j-1} \times (F_{Y_{l:K}}(v_j) - F_{Y_{l:K}}(v_{j-1})), \quad (47a)$$

and for $\bar{H} \geq K\xi q/(RT_s)$, we find $\sup_{\frac{N\bar{H}R}{Kq} < P < \infty} \mathbb{E}[\hat{Y}_{\text{meas}}]$

$$= e^{-\frac{K\xi q}{\bar{H}T_s R}} \sum_{l=1}^K \left(1 - e^{-\frac{K\xi q}{\bar{H}T_s R}}\right)^{K-l} \sum_{j=1}^{2^q} v_{j-1} \times (F_{Y_{l:K}}(v_j) - F_{Y_{l:K}}(v_{j-1})). \quad (47b)$$

We compare (45), (46), and (47) to get $\sup_{P \geq 0} \mathbb{E}[\hat{Y}_{\text{meas}}]$.

i) When $\bar{H} \geq K\xi q/(RT_s)$: The expression for the supremum of $\mathbb{E}[\hat{Y}_{\text{meas}}]$ over $0 \leq P \leq N\bar{H}R/(Kq)$ from (45) and (46) is the same as that over $N\bar{H}R/(Kq) < P < \infty$. Thus, it is the expression for the supremum of $\mathbb{E}[\hat{Y}_{\text{meas}}]$ over $P \geq 0$, and is given by (13a). It is achieved at $P_{K,q}^* = N\bar{H}R/(Kq)$.

ii) When $\bar{H} < K\xi q/(RT_s)$: From (45), (46), and (47), it follows that $\sup_{\frac{N\bar{H}R}{Kq} < P < \infty} \mathbb{E}[\hat{Y}_{\text{meas}}] > \sup_{0 \leq P \leq \frac{N\bar{H}R}{Kq}} \mathbb{E}[\hat{Y}_{\text{meas}}]$. Hence, $\sup_{P \geq 0} \mathbb{E}[\hat{Y}_{\text{meas}}]$ is given by (13b) and is achieved at $P_{K,q}^* = N\xi/T_s$.

D. Brief Proof of Theorem 4

Let ζ be the probability that a node has sufficient transmit and CSI acquisition energy. Now, the average energy consumed by a node in a DCR in the with-CSI model for transmitting q -bit readings is $\bar{U} = \frac{K}{N}\zeta \left(cT_f + \frac{qP}{R}\psi\right)$. This is because a scheduled node has energy $cT_f + \frac{qP}{R}$ with probability ζ . In this event, it uses cT_f energy for channel estimation. And, it transmits with energy $\frac{qP}{R}$ only when its channel gain exceeds $\omega\eta k_B \Delta W/P$, which happens with probability ψ .

As in Appendix B, we calculate the sup $\mathbb{E}[\hat{Y}_{\text{meas}}]$ separately for $\bar{H} < KcT_f/N$ and $\bar{H} \geq KcT_f/N$.

1) When $\bar{H} < KcT_f/N$: Following steps similar to Appendix B1, it can be shown that $\zeta < 1$ and $\bar{H} = \bar{U}$. Therefore, $\bar{H} = \bar{U} = \frac{K}{N}\zeta \left(cT_f + \frac{qP}{R}\psi\right)$. Rearranging terms and substituting $\psi = e^{-\frac{N\xi}{P T_s}}$ (cf. (17)), we get $\zeta\psi = \frac{N\bar{H}}{K \left(cT_f + \frac{qP}{R} e^{-\frac{N\xi}{P T_s}}\right)} e^{-\frac{N\xi}{P T_s}}$. $\mathbb{E}[\hat{Y}_{\text{meas}}]$ is increasing in $\zeta\psi$ (cf. Appendix C3). Using steps similar to Appendix B1, it can be shown that $\zeta\psi$ and, hence, $\mathbb{E}[\hat{Y}_{\text{meas}}]$ achieve their supremum at $P = N\xi/(2T_s\Omega'_2)$. Substituting this in (42) yields the expression for $\sup_{P \geq 0} \mathbb{E}[\hat{Y}_{\text{meas}}]$ in (15b).

2) When $\bar{H} \geq KcT_f/N$: We evaluate the sup $\mathbb{E}[\hat{Y}_{\text{meas}}]$ in the following three regimes: i) $0 \leq P < N\xi/(T_s\Omega'_1)$, ii) $P = N\xi/(T_s\Omega'_1)$, and iii) $N\xi/(T_s\Omega'_1) < P < \infty$. Across them, the system switches from being energy unconstrained to energy constrained.

i) When $0 \leq P < N\xi/(T_s\Omega'_1)$: Using steps similar to Appendix B2, it can be shown that $\zeta = 1$. As shown in Appendix C1, $\mathbb{E}[\hat{Y}_{\text{meas}}]$ is monotonically increasing in ψ . Furthermore, since P lies in between 0 and $\frac{N\xi}{T_s\Omega'_1}$, ψ lies in between 0 and $e^{-\Omega'_1}$. Therefore, from (44), we get

$$\sup_{0 \leq P < \frac{N\xi}{T_s\Omega'_1}} \mathbb{E}[\hat{Y}_{\text{meas}}] = e^{-\Omega'_1} \sum_{l=1}^K \left(1 - e^{-\Omega'_1}\right)^{K-l} \times \sum_{j=1}^{2^q} v_{j-1} (F_{Y_{l:K}}(v_j) - F_{Y_{l:K}}(v_{j-1})), \quad (48)$$

which occurs as $P \rightarrow \left(\frac{N\xi}{T_s\Omega'_1}\right)^-$.

ii) When $P = N\xi/(T_s\Omega'_1)$: Similar to Footnote 7, it can be shown here that $\zeta = 1$. Substituting this in (17) we get $\psi = e^{-\Omega'_1}$. Substituting these values, in turn, in (42), we get

$$\mathbb{E}[\hat{Y}_{\text{meas}}] = e^{-\Omega'_1} \sum_{l=1}^K \left(1 - e^{-\Omega'_1}\right)^{K-l} \times \sum_{j=1}^{2^q} v_{j-1} (F_{Y_{l:K}}(v_j) - F_{Y_{l:K}}(v_{j-1})). \quad (49)$$

iii) When $N\xi/(T_s\Omega'_1) < P < \infty$: Using steps similar to those in Appendix B2, we find that $\zeta < 1$. As shown in Appendix C3, for $\zeta < 1$, $\mathbb{E}[\hat{Y}_{\text{meas}}]$ is monotonically increasing in $\zeta\psi$, whose supremum can be shown to be different for $\Omega'_1 > 2\Omega'_2$ and for $\Omega'_1 \leq 2\Omega'_2$.

If $\Omega'_1 > 2\Omega'_2$, it can be shown along lines similar to Appendix B2 that

$$\sup_{\frac{N\xi}{T_s\Omega'_1} < P < \infty} \mathbb{E}[\hat{Y}_{\text{meas}}] = \sigma'_2 \sum_{l=1}^K (1 - \sigma'_2)^{K-l} \times \sum_{j=1}^{2^q} v_{j-1} (F_{Y_{l:K}}(v_j) - F_{Y_{l:K}}(v_{j-1})), \quad (50)$$

and the supremum is achieved at $P = N\xi/(2T_s\Omega'_2)$. If $\Omega'_1 \leq 2\Omega'_2$, as in Appendix B2, we can show that

$$\sup_{\frac{N\xi}{T_s\Omega'_1} < P < \infty} \mathbb{E}[\hat{Y}_{\text{meas}}] = e^{-\Omega'_1} \sum_{l=1}^K \left(1 - e^{-\Omega'_1}\right)^{K-l} \times \sum_{j=1}^{2^q} v_{j-1} (F_{Y_{l:K}}(v_j) - F_{Y_{l:K}}(v_{j-1})), \quad (51)$$

and the supremum is achieved as $P \rightarrow \left(\frac{N\xi}{T_s\Omega'_1}\right)^+$.

Combining (48) and (49), we get

$$\sup_{0 \leq P \leq \frac{N\xi}{T_s\Omega'_1}} \mathbb{E}[\hat{Y}_{\text{meas}}] = e^{-\Omega'_1} \sum_{l=1}^K \left(1 - e^{-\Omega'_1}\right)^{K-l} \times \sum_{j=1}^{2^q} v_{j-1} (F_{Y_{l:K}}(v_j) - F_{Y_{l:K}}(v_{j-1})). \quad (52)$$

We determine $\sup_{0 \leq P < \infty} \mathbb{E}[\hat{Y}_{\text{meas}}]$ based on the above results as follows.

a) If $\Omega'_1 > 2\Omega'_2$: From the discussion following (50), since $P = N\xi/(2T_s\Omega'_2)$ is the optimal power and not $P = N\xi/(T_s\Omega'_1)$, we find that $\sup_{\frac{N\xi}{T_s\Omega'_1} < P < \infty} \mathbb{E}[\hat{Y}_{\text{meas}}]$ is greater than $\mathbb{E}[\hat{Y}_{\text{meas}}]$ when $P = N\xi/(T_s\Omega'_1)$. The latter is also the supremum of $\mathbb{E}[\hat{Y}_{\text{meas}}]$ over $0 \leq P \leq N\xi/(T_s\Omega'_1)$ (cf. (52)). Therefore, $\sup_{\frac{N\xi}{T_s\Omega'_1} < P < \infty} \mathbb{E}[\hat{Y}_{\text{meas}}] > \sup_{0 \leq P \leq \frac{N\xi}{T_s\Omega'_1}} \mathbb{E}[\hat{Y}_{\text{meas}}]$.

Therefore, $\sup_{0 \leq P < \infty} \mathbb{E}[\hat{Y}_{\text{meas}}]$ is given by (15b), and is achieved at $P_{K,q}^* = N\xi/(2T_s\Omega'_2)$.

b) If $\Omega'_1 \leq 2\Omega'_2$: We find that the expressions for the supremum of $\mathbb{E}[\hat{Y}_{\text{meas}}]$ over $0 \leq P \leq N\xi/(T_s\Omega'_1)$ in (52) and $P > N\xi/(T_s\Omega'_1)$ in (51) are the same. Hence, $\sup_{P \geq 0} \mathbb{E}[\hat{Y}_{\text{meas}}]$ is given by (15a), and is achieved at $P_{K,q}^* = N\xi/(T_s\Omega'_1)$.

ACKNOWLEDGMENT

The authors would like to thank Prof. Vinod Sharma, IISc, for inputs regarding the stability of the G/G/1 queue.

REFERENCES

[1] I. F. Akyildiz, T. Melodia, and K. R. Chowdury, "Wireless multimedia sensor networks: A survey," *IEEE Wireless Commun.*, vol. 14, no. 6, pp. 32–39, Dec. 2007.

[2] A. Giridhar and P. Kumar, "Toward a theory of in-network computation in wireless sensor networks," *IEEE Commun. Mag.*, vol. 44, no. 4, pp. 98–107, Apr. 2006.

[3] A. Giridhar and P. Kumar, "Computing and communicating functions over sensor networks," *IEEE J. Sel. Areas Commun.*, vol. 23, no. 4, pp. 755–764, Apr. 2005.

[4] N. Khude, A. Kumar, and A. Karnik, "Time and energy complexity of distributed computation of a class of functions in wireless sensor networks," *IEEE Trans. Mobile Comput.*, vol. 7, no. 5, pp. 617–632, May 2008.

[5] A. Anand and N. Mehta, "Quick, decentralized, energy-efficient one-shot max function computation using timer-based selection," *IEEE Trans. Commun.*, vol. 63, no. 3, pp. 927–937, Mar. 2015.

[6] M. Li, Y. Wang, and Y. Wang, "Complexity of data collection, aggregation, and selection for wireless sensor networks," *IEEE Trans. Comput.*, vol. 60, no. 3, pp. 386–399, Mar. 2011.

[7] I. Dietrich and F. Dressler, "On the lifetime of wireless sensor networks," *ACM Trans. Sens. Netw.*, vol. 5, no. 1, pp. 1–39, Feb. 2009.

[8] G. Riva, J. Finochietto, and G. Leguizamón, "Bio-inspired in-network filtering for wireless sensor monitoring systems," in *Proc. IEEE CEC*, Jun. 2013, pp. 3379–3386.

[9] V. Sharma, U. Mukherji, V. Joseph, and S. Gupta, "Optimal energy management policies for energy harvesting sensor nodes," *IEEE Trans. Wireless Commun.*, vol. 9, no. 4, pp. 1326–1336, Apr. 2010.

[10] K. Ramachandran and B. Sikdar, "A population based approach to model the lifetime and energy distribution in battery constrained wireless sensor networks," *IEEE J. Sel. Areas Commun.*, vol. 28, no. 4, pp. 576–586, Apr. 2010.

[11] B. Medepally and N. B. Mehta, "Voluntary energy harvesting relays and selection in cooperative wireless networks," *IEEE Trans. Wireless Commun.*, vol. 9, no. 11, pp. 3543–3553, Nov. 2010.

[12] S. Cui, J.-J. Xiao, A. Goldsmith, Z.-Q. Luo, and H. Poor, "Estimation diversity and energy efficiency in distributed sensing," *IEEE Trans. Signal Process.*, vol. 55, no. 9, pp. 4683–4695, Sep. 2007.

[13] C. Huang, Y. Zhou, T. Jiang, P. Zhang, and S. Cui, "Power allocation for joint estimation with energy harvesting constraints," in *Proc. ICASSP*, May 2013, pp. 4804–4808.

[14] F. Iannello, O. Simeone, and U. Spagnolini, "Medium access control protocols for wireless sensor networks with energy harvesting," *IEEE Trans. Commun.*, vol. 60, no. 5, pp. 1381–1389, May 2012.

[15] Zigbee, *IEEE Standard for Local and Metropolitan Area Networks*, IEEE Std 802.15.4e-2012 (Amendment to IEEE Std 802.15.4-2011).

[16] Y. Zhao, B. Chen, and R. Zhang, "Optimal power allocation for an energy harvesting estimation system," in *Proc. ICASSP*, May 2013, pp. 4549–4553.

[17] J. Wu and G. Zhou, "A new ultra-low power wireless sensor network with integrated energy harvesting, data sensing, and wireless communication," in *Proc. ICC*, Jun. 2011, pp. 1–5.

[18] L. Vijayandran, M. Brandt-Pearce, K. Kansanen, and T. Ekman, "Efficient state estimation with energy harvesting and fairness control using stochastic optimization," in *Proc. IEEE Globecom*, Dec. 2011, pp. 1–6.

[19] R. Corless, G. Gonnet, D. Hare, D. Jeffrey, and D. Knuth, "On the LambertW function," *Adv. Comp. Math.*, vol. 5, no. 1, pp. 329–359, 1996. [Online]. Available: <http://dx.doi.org/10.1007/BF02124750>

[20] B. C. Arnold, N. Balakrishnan, and H. N. Nagaraja, *A First Course in Order Statistics*. Philadelphia, PA, USA: SIAM, 2008.

[21] K. Huang, "Spatial throughput of mobile ad hoc networks powered by energy harvesting," *IEEE Trans. Inf. Theory*, vol. 59, no. 11, pp. 7597–7612, Nov. 2013.

[22] A. J. Goldsmith, *Wireless Communications*, 1st ed. Cambridge, U.K.: Cambridge Univ. Press, 2005.

[23] R. Niu, B. Chen, and P. Varshney, "Fusion of decisions transmitted over Rayleigh fading channels in wireless sensor networks," *IEEE Trans. Signal Process.*, vol. 54, no. 3, pp. 1018–1027, Mar. 2006.

[24] H. Ju and R. Zhang, "Throughput maximization in wireless powered communication networks," *IEEE Trans. Wireless Commun.*, vol. 13, no. 1, pp. 418–428, Jan. 2014.

[25] HART Communication Foundation. [Online]. Available: http://en.hartcomm.org/hcf/org_mbr/documents/documents_spec_list.html

[26] ISA 100.11a. [Online]. Available: <https://www.isa.org/standards-and-publications/isa-standards/>

[27] P. Loh, Y. Pan, and H. Jing, "Performance evaluation of efficient and reliable routing protocols for fixed-power sensor networks," *IEEE Trans. Wireless Commun.*, vol. 8, no. 5, pp. 2328–2335, May 2009.

[28] F. Baccelli and P. Brémaud, *Elements of Queuing Theory: Palm-Martingale Calculus and Stochastic Recurrences*, ser. Applications of mathematics. Stochastic modelling and applied probability, New York, NY, USA: Springer-Verlag, 1994.

[29] B. Medepally, N. B. Mehta, and C. R. Murthy, "Implications of energy profile and storage on energy harvesting sensor link performance," in *Proc. IEEE Globecom*, Dec. 2009, pp. 1695–1700.



Shilpa Rao received the B.Eng. degree in electronics and communication engineering from Sri Jayachamarajendra College of Engineering, Mysore, India, in 2006. From 2006–2009, she was at Toshiba Software (India) Pvt. Ltd., working on software development for video codecs. She is currently pursuing the Ph.D. degree in the Department of Electrical Communication Engineering, Indian Institute of Science (IISc). Her research interests include design and analysis of energy harvesting wireless sensor networks.



Neelesh B. Mehta (S'98–M'01–SM'06) received the B.Tech. degree in electronics and communications engineering from the Indian Institute of Technology (IIT), Madras, India, in 1996, and the M.S. and Ph.D. degrees in electrical engineering from the California Institute of Technology, Pasadena, CA, USA, in 1997 and 2001, respectively. He is now an Associate Professor in the Department of Electrical Communication Engineering, Indian Institute of Science (IISc), Bangalore, India. He serves as an Executive Editor of the IEEE TRANSACTIONS ON WIRELESS COMMUNICATIONS, and as an Editor of the IEEE TRANSACTIONS ON COMMUNICATIONS and IEEE WIRELESS COMMUNICATION LETTERS. He served as the Director of Conference Publications on the Board of Governors of the IEEE ComSoc in 2012–2013 and currently serves as a Member-at-Large on the Board.